A01-25107

42nd AIAA/ASME/ASCE/AHS/ASC Structures, Structural Dynamics, and Materials Conference and Exhibit
Seattle, WA 16-19 April 2001

AIAA-2001-1328

# REFINED DESIGN CURVES FOR COMPRESSIVE BUCKLING OF CURVED PANELS USING NONLINEAR FINITE ELEMENT ANALYSIS

Moshe M. Domb* and Barry R. Leigh†
Bombardier Aerospace
Strategic Technology Group
123 Garratt Blvd., Downsview, Ontario
Canada, M3K 1Y5



## ABSTRACT

The present work deals with implementation of a non-linear finite element technique for the prediction of the initial buckling in simply-supported curved panels subjected to pure compression. A single nonlinear design curve is derived, representing the compressive buckling stress coefficient as a function of the curved panel parameter for a radius-to-thickness ratio between 1000 and 2000. The proposed curve represents an update and expansion of the currently-used NACA design curves, and it includes the effect of a pre-existing level of imperfection in the panel on the buckling coefficient.The results presented in this work show a strong dependency of the buckling stress on the degree of initial imperfection in the panel, especially for highly-curved panels. The results also indicate that the actual amount of imperfection in a given panel is dependent upon the curved panel parameter and its radius-to-thickness ratio. A detailed knowledge of this dependency would lead to a better prediction of the buckling stress of the panel.

## INTRODUCTION

### The NASA Structural Stability Monographs

The current sources of design information on the stability of shell structures are the Structures Monographs published by the National Aeronautics and Space Administration (NASA) in the 1960's.[1-3] These monographs provide design information in the form of empirical knockdown factors and design recommendations for isotropic flat and curved panels. The factors represent lower bounds to experimental data available at that time, and they take into account the large scatter obtained in the test data. These corrections are done to account primarily for the high sensitivity of shell buckling to initial geometric imperfections in the structure. The NASA structural stability monographs and all the references from the 1940's and 1950's on which the monographs are based, provide a reliable but over-conservative means of designing shells structures. The amount of information given is limited and its applicability to high-performance shell structures, such as fibre-reinforced composite structures, is small. The design guidelines on shell stability given in the NASA monographs are widely used throughout the aerospace industry.

Many advances in the area of shell stability analysis have been accomplished since the days of the NASA monographs. At the same time, the availability today of modern and affordable computing resources has enabled the development of advanced computational structural analysis capabilities for the nonlinear analysis of shell structures. As a result, it can be concluded that the information provided in the NASA monographs on shell stability, as it has also been indicated in Reference 4, can and need to be updated and expanded.

### Current Approach and Objective

The currently-used design curves for the critical compressive buckling stress coefficients of simply-supported and clamped curved panels are presented in Figure 1, after the original source by NACA.[5] The figure depicts the compressive buckling stress coefficient $k_c$ as a function of the curved panel parameter $Z_b$ for a wide range of radius-to-thickness ratios. The expressions for $k_c$ and $Z_b$ are given by:

$$k_c = \frac{12(1-\nu^2)}{\pi^2 E}\left(\frac{b}{t}\right)^2 F_c^{cr} \qquad (1)$$

and

$$Z_b = \frac{b^2}{rt}\sqrt{1-\nu^2} \quad , \qquad (2)$$

where $E, \nu, b, t, r, F_c^{cr}$ are the panel Young's modulus, Poisson's ratio, width (circumferential dimension),

*Ph.D., mdomb@dehavilland.ca

†bleigh@dehavilland.ca

thickness, radius and critical compressive stress, respectively. These design curves represent the minima of highly-scattered test data gathered in the 1940's. A description regarding the test data and their respective sources can be found in References 5-8.

A nonlinear finite element technique for the buckling analysis of curved panels has been developed at Bombardier Aerospace. The present work deals with implementation of this technique for the prediction of the initial buckling in simply-supported curved panels subjected to pure compression. The current approach includes the effect of a pre-existing level of imperfection in the panel on the buckling coefficient. The software used here is the Finite Element Analysis code MARC, a commercial package known for its advanced nonlinear capabilities. The objective is to generate refined design curves which will represent an update and expansion of the currently-used NACA design curves.

## MODEL DESCRIPTION

A schematic view of a typical curved panel configuration together with its general dimensions is presented below. In the selection of the panels to be analyzed, a number of geometric and material parameters are preselected and kept constant for all panels. These parameters are the panel's radius $r$, thickness $t$, aspect ratio $a/b$, Young's modulus $E$ and Poisson's ratio $\nu$. Specification of the curved panel parameter $Z_b$ for the different panels subsequently determines the value of the corresponding panel width $b$ (via Eq. 2) and panel length $a$.

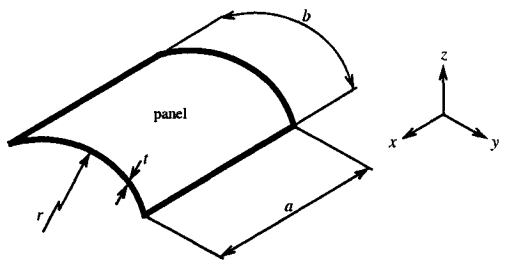


The compressive loading is applied incrementally via prescribed uniform displacement in the axial direction of the panel. Incorporation of initial geometric imperfections in the panel is done through a coordinate perturbation in the radial direction of the panel for each node in the finite element model. The perturbation is specified as a linear combination of the first four buckling modes of the panel obtained from a linear eigenvalue buckling solution.[9] The initial radial displacement $\Delta r_0$ at node $n$ is therefore given by

$$\Delta r_0(n) = \sum_{i=1}^{4} c_i r_{0i}(n) \qquad (3)$$

where $r_{0i}$ are the nodal displacements in the radial direction for the individual mode shapes, and $c_i$ are pre-specified weighting factors. The initial radial displacement distribution $\Delta r_0$ is then normalized with respect to the largest radial displacement within the panel in order to ensure a maximum non-dimensional radial displacement value of one. The largest initial radial displacement $\Delta r_{0max}$ is given by

$$\Delta r_{0max} = max\,[\Delta r_0(n)] \quad . \qquad (4)$$

In addition, the normalized radial displacement distribution is pre-multiplied by the panel thickness $t$ and a pre-defined imperfection coefficient $a_0$. This representation allows the specification of the largest amplitude as a fraction of the nominal panel thickness via the coefficient $a_0$. As a result, the radial perturbation $\Delta r$ applied at each node in the model can be written as:

$$\Delta r(n) = a_0 t \frac{\Delta r_0(n)}{\Delta r_{0max}} \quad . \qquad (5)$$

### Determination of the Buckling Load

The techniques typically used for the identification of the instant of buckling in panels under compression loading are strongly dependent upon the global response of the panel during the loading procedure, which by itself depends on the specific configuration of the panel. For this purpose, three typical cases have been identified in the current work, and they are depicted schematically in Figure 2.

The most straightforward approach would be identification of the instant of buckling directly from the panel's overall load-versus-displacement curve (or stress-versus-strain curve). One case of this kind of response, referred to as Case I, is characterized by an overall bilinear load-displacement dependency. The point of discontinuity in the slope represents the instant of buckling of the panel. A second case under the same approach, referred to as Case II, exhibits a very gradual reduction in stiffness (an almost linear curve) even at small load levels, followed by a sudden drop in the load. The peak load clearly represents the buckling load of the panel.

It should be noted that the curve for Case II exhibits a peculiar behaviour in the post-buckled region, in which the prescribed displacement loading is being reduced

during the incremental procedure. This is a result of the incremental load option used in the current analysis, which allows for an automatic load stepping procedure in a quasi-static fashion. During such an loading session, and in the process of searching for a converged state, the program may encounter such an instability that reduces the load rather than the desired load addition. In order to avoid this phenomenon, a user-defined incremental loading procedure can be used. For the purpose of identifying the instant of buckling, as in the case of the current study, either incremental procedure can be used with generally similar results.

Unlike the first two cases described above, some panel configurations are characterized by a load-displacement curve which exhibits a nonlinear response immediately from the onset of loading, with a continuous reduction in the overall stiffness (Case III in Figure 2). In such a case, the critical buckling load cannot be pinpointed directly from an inspection of the load-deflection curve. Therefore, a different procedure must be applied. In this case, the development of the out-of-plane displacement as a function of the applied displacement loading is followed at the location in the panel which displays the largest deflection at the post-buckled stage. In mathematical terms, the instant of buckling for this case is identified when:

$$\left[\frac{\partial w_{cr}}{\partial u_o}\right] = maximum \qquad (6)$$

where $w_{cr}, u_o$ are the out-of-plane deflection of the critical location in the panel and the applied displacement loading, respectively.

## MODEL RESULTS AND DISCUSSION

The panels analyzed correspond to the cases of radius-to-thickness ratios of 1000 and 2000, and are in the range of curved panel parameter of $0 \le Z_b \le 200$. The above range of radius-to-thickness ratio was selected because it represents the range where most curved panels used in current aircraft structures are contained (see Table 1). The complete set of geometric and material data for the panels analyzed here are given in Table 2.

Plots related to three representative configurations for the case $r/t$=1000 are presented here. These correspond to panels with $Z_b$=5, 30 and 100. Typical post-buckled shapes for these panels and the predictions of the compressive stress-versus-strain curves for several values of $a_0$ are shown in Figure 3 to Figure 8. The reference buckling stress predictions based on the current NACA design curves are also shown.

Model results for the buckling stress coefficient $k_c$ for all the panels analyzed are depicted in Figure 9 and Figure 10 in a $k_c$ vs. $Z_b$ plot as a function of the imperfection coefficient $a_0$. The NACA theoretical and design curves[5], and a set of experimental data points[10-12] are also shown. The range for $Z_b$ typical of curved panels used today in aircraft structures is also outlined. It can be seen in all panels analyzed that, as expected, the predicted buckling stress coefficient for a given panel configuration (i.e. for a particular value of $Z_b$) drops as the value of the imperfection in the panel is increased. The predictions fall well within the scatter of the test data.

The overall range of curved panels can be divided into three main regions: flat range ( $0 \le Z_b < 7$ ), intermediate range ( $7 \le Z_b \le 25$ ) and highly-curved range ( $25 < Z_b$ ). The nonlinear results for curved panels corresponding to the flat and intermediate regions correlate well with the current NACA design estimates for values of $a_0 \le 0.05$. It should be noted that from practical manufacturing considerations, curved panels in these two regions are characterized by very low levels of imperfection. Therefore, it seems logical that the proposed design curve for the flat and intermediate range of panels should in fact duplicate the NACA design curve. For panels in the highly-curved range, the nonlinear results lie above the design curve for all the levels of imperfection investigated. Panels in this range are characterized by an imperfection level believed to be in the range $0.20 \le a_0 \le 0.50$, which is larger than that for panels in the flat and intermediate regions. Considering that the dependency of the imperfection parameter $a_0$ on the curved panel parameter $Z_b$ has not yet been quantified, it is reasonable at this point to represent the panels in this range by the nonlinear curve with $a_0$=0.20.

The predicted $k_c$-versus-$Z_b$ curves for panels with $r/t = 1000$ and 2000 for an imperfection coefficient of $a_0$=0.20 are depicted in Figure 11 together with the current NACA design curves. It can be seen that, although NACA shows a distinction between the curves for the above $r/t$ ratios, the nonlinear model curves for these ratios were found to be essentially identical. This difference could be a consequence of the fact that the model results for the above $r/t$ ratios are given for the case $a_0$=0.20, while the NACA curves are believed to reflect a dependence of $a_0$ on the $r/t$ ratio for a given panel (larger initial imperfections in panels with larger $r/t$ ratios). As a result, the nonlinear curve for the case $r/t$=1000 in the highly-curved range has been selected for the purpose of defining a single nonlinear design curve.

A single nonlinear design curve, depicted in Figure 12 by the solid line, is generated in the range $1 \le Z_b \le 200$ for simply-supported curved panels with *r/t* ratio between 1000 and 2000. This curve duplicates the original NACA design curve in the range $1 \le Z_b < 23.15$, while for $23.15 \le Z_b \le 200$ it represents a curve-fit to the nonlinear results for the case $r/t = 1000$ with $a_0$=0.20. The mathematical definition of the proposed curve for the range r/t=1000 to 2000 is given in the following equation:

$$k_c(Z_b) = \begin{cases} 10^{\sum_{i=0}^{3} c_i (\log Z_b)^i} & ; \quad 1 \le Z_b < 23.15 \\ c\,(Z_b)^d & ; \quad 23.15 \le Z_b \le 200 \end{cases} \quad (7)$$

where $c_0$=0.6021, $c_1$=0.005377, $c_2$=0.192495, $c_3$=-0.002670, $c$=0.4323 and $d$=0.9748. The effect of the level of imperfection in the panel on the buckling coefficient is embedded into this single design curve.

## CONCLUDING REMARKS

Implementation of a nonlinear buckling analysis technique for the prediction of the initial buckling in simply-supported curved panels subjected to pure compression has been presented. It is believed that the currently-used NACA design curves are conservative when applied to panels in the highly-curved range. A single nonlinear design curve was generated in the current study, representing the compressive buckling stress coefficient $k_c$ as a function of the curved panel parameter $Z_b$ with radius-to-thickness ratio between 1000 and 2000 (the range typical of curved panels used in current aircraft structures). The proposed curve represents an update and expansion of the NACA curves, and it includes the effect of a pre-existing level of imperfection in the panel on the buckling coefficient.

The results presented in this work show a strong dependency of the buckling stress on the degree of initial imperfection in curved panels, especially for panels in the intermediate and highly-curved ranges. These results also indicate that the actual amount of imperfection in a given panel is dependent upon the curved panel parameter $Z_b$ as well as on its *r/t* ratio. A detailed knowledge of this dependency would lead to a better prediction of the buckling stress of the panel.

## REFERENCES

[1]Anon., "Buckling of Thin-Walled Circular Cylinders", NASA Space Vehicle Design Criteria (Structures), NASA SP-8007, September 1965.

[2]Anon., "Buckling of Thin-Walled Truncated Cones", NASA Space Vehicle Design Criteria (Structures), NASA SP-8019, September 1968.

[3]Anon., "Buckling of Thin-Walled Doubly-Curved Shells", NASA Space Vehicle Design Criteria (Structures), NASA SP-8032, August 1969.

[4]Nemeth, M. P. and Starnes Jr., J. H., "The NASA Monographs on Shell Stability Design Recommendations - A Review and Suggested Improvements", NASA TP-1998-206290, January 1998.

[5]Batdorf, S. B., Schildcrout, M. and Stein, M., "Critical Combinations of Shear and Longitudinal Direct Stress for Long Plates with Transverse Curvature", NACA TN-1347, June 1947.

[6]Gerard, G. and Becker, H., "Handbook of Structural Stability. Part III - Buckling of Curved Plates and Shells", NACA TN-3783, August 1957.

[7]Batdorf, S. B., Schildcrout, M. and Stein, M., "Critical Shear Stress of Long Plates with Transverse Curvature", NACA TN-1346, June 1947.

[8]Batdorf, S. B., Stein, M. and Schildcrout, M., "Critical Shear Stress of Curved Rectangular Plates", NACA TN-1348, May 1947.

[9]Sobel, L. and Sharp, D., "Comparison of Analytical and Experimental Results for the Postbuckling Behavior of a Stiffened Flat Composite Shear Panel", Proceedings of the 35th AIAA/ASME/ASCE/AHS/ASC Structures, Structural Dynamics and Materials Conference, April 18-20 1994, Hilton Head, SC, USA, pp.449-457.

[10]Cox, H. L. and Clenshaw, W. J., "Compression Tests on Curved Plates of Thin Sheet Duralumin", Reports & Memoranda No. 1894, British Aeronautical Research Committee, November 1941.

[11]Crate, H. and Levin, L. R., "Data on Buckling Strength of Curved Sheet in Compression", NACA WR L-557 (formerly NACA ARR-3J04), 1943.

[12]Jackson, K. V. and Hall, A. H., "Curved Plates in Compression", Report AR-1 (MM-180), National Research Council, 1947.

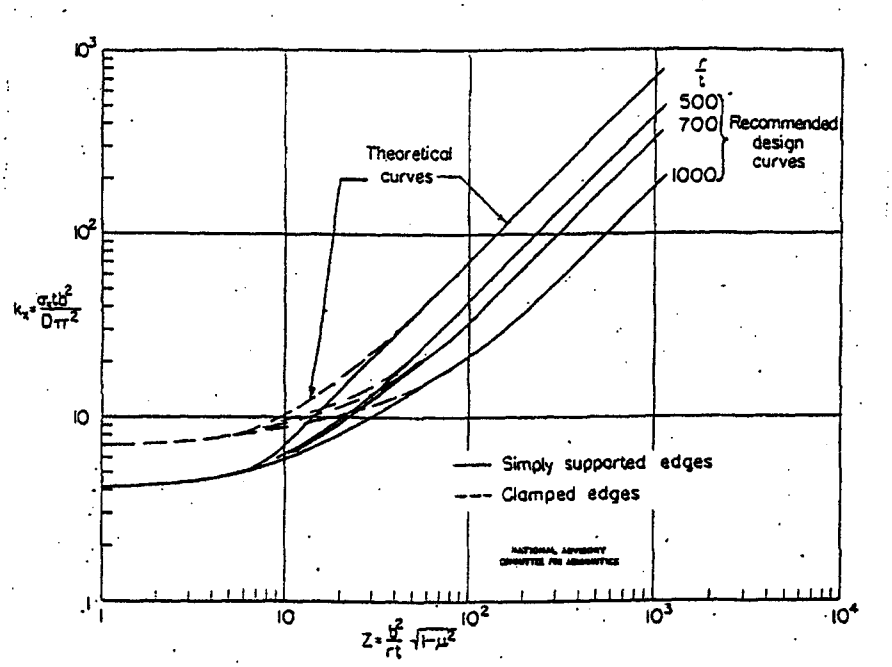


**Figure 1:** Theoretical and Design Critical Compressive buckling stress coefficients for Long Curved Panels with Simply-Supported and Clamped Edges [5].

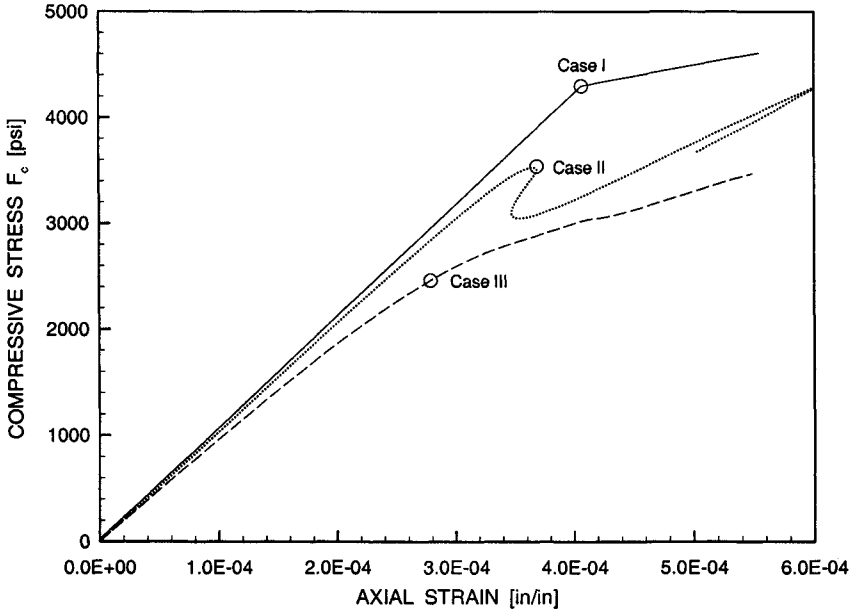


**Figure 2:** The Various Cases Encountered in the Prediction of the Compressive Stress-versus-Strain Curve for a Simply-Supported Curved Panel, and the Identification of the Corresponding Buckling Stress.

**Table 1:** Fuselage Information from Various Transport Aircraft.

| Aircraft | *max. r* | *min. t* | *b* | *a* | $Z_b$ | *r/t* |
|---|---|---|---|---|---|---|
| | [in] | [in] | [in] | [in] | ----- | ----- |
| A310 | 111 | 0.063 | ~ 9.0 | 20 | 10.9 | 1762 |
| B737 | 74 | 0.036 | ~ 9.0 | 20 | 28.7 | 2056 |
| B747 | 128 | 0.071 | 9.5 | 20 | 9.4 | 1803 |
| B757 | 74 | 0.040 | ~ 9.0 | 20 | 25.8 | 1850 |
| C-141 | 85 | 0.053 | 6.0 | 20 | 7.5 | 1604 |
| Concord | 56 | 0.055 | ~ 9.0 | 21 | 24.6 | 1027 |
| DC-8 | 73 | 0.050 | 7.2 | 20 | 13.3 | 1470 |
| DC-10 | 118 | 0.071 | 8.0 | 20 | 7.2 | 1669 |
| DHC-8 | 53 | 0.028 | 5.2 | 21 | 17.2 | 1893 |
| L-1011 | 117 | 0.075 | 9.0 | 20 | 8.7 | 1567 |

**Table 2:** Geometric and Material Data of the Panels Analyzed.

| r/t | *E* | *n* | *r* | *t* | *b* | *a=4b* | $Z_b$ | $k_c^{naca}$ | $F_c^{naca}$ |
|---|---|---|---|---|---|---|---|---|---|
| | [Msi] | ----- | [in] | [in] | [in] | [in] | ----- | ----- | [psi] |
| Flat | 10.5 | 0.33 | • | 0.030 | 5.000 | 20.000 | 0 | 4.0 | 1395.5 |
| 1000 | 10.5 | 0.33 | 30 | 0.030 | 1.381 | 5.524 | 2 | 4.2 | 19211.6 |
| | | | | | 1.691 | 6.765 | 3 | 4.5 | 13722.6 |
| | | | | | 2.183 | 8.733 | 5 | 5.0 | 9148.4 |
| | | | | | 2.583 | 10.334 | 7 | 5.5 | 7188.0 |
| | | | | | 3.088 | 12.351 | 10 | 6.2 | 5672.0 |
| | | | | | 3.782 | 15.127 | 15 | 7.5 | 4574.2 |
| | | | | | 4.367 | 17.467 | 20 | 8.5 | 3888.1 |
| | | | | | 5.348 | 21.392 | 30 | 10.5 | 3201.9 |
| | | | | | 6.175 | 24.702 | 40 | 12.5 | 2858.9 |
| | | | | | 6.904 | 27.618 | 50 | 14.3 | 2616.4 |
| | | | | | 7.563 | 30.253 | 60 | 16.0 | 2439.6 |
| | | | | | 8.169 | 32.677 | 70 | 17.7 | 2313.2 |
| | | | | | 8.733 | 34.934 | 80 | 19.5 | 2229.9 |
| | | | | | 9.263 | 37.053 | 90 | 21.0 | 2134.6 |
| | | | | | 9.764 | 39.057 | 100 | 23.0 | 2104.1 |
| | | | | | 13.809 | 55.235 | 200 | 40.0 | 1829.7 |
| 2000 | 10.5 | 0.33 | 60 | 0.030 | 1.953 | 7.811 | 2 | 4.2 | 9605.8 |
| | | | | | 2.392 | 9.567 | 3 | 4.5 | 6861.3 |
| | | | | | 3.088 | 12.351 | 5 | 5.0 | 4574.2 |
| | | | | | 3.653 | 14.614 | 7 | 5.5 | 3594.0 |
| | | | | | 4.367 | 17.467 | 10 | 6.2 | 2836.0 |
| | | | | | 5.348 | 21.392 | 15 | 7.5 | 2287.1 |
| | | | | | 6.175 | 24.702 | 20 | 8.5 | 1944.0 |
| | | | | | 7.563 | 30.253 | 30 | 10.2 | 1555.2 |
| | | | | | 8.733 | 34.934 | 40 | 12.0 | 1372.3 |
| | | | | | 10.696 | 42.785 | 60 | 15.0 | 1143.5 |
| | | | | | 12.351 | 49.404 | 80 | 18.0 | 1029.2 |
| | | | | | 13.809 | 55.235 | 100 | 21.0 | 960.6 |
| | | | | | 19.529 | 78.114 | 200 | 36.0 | 823.3 |

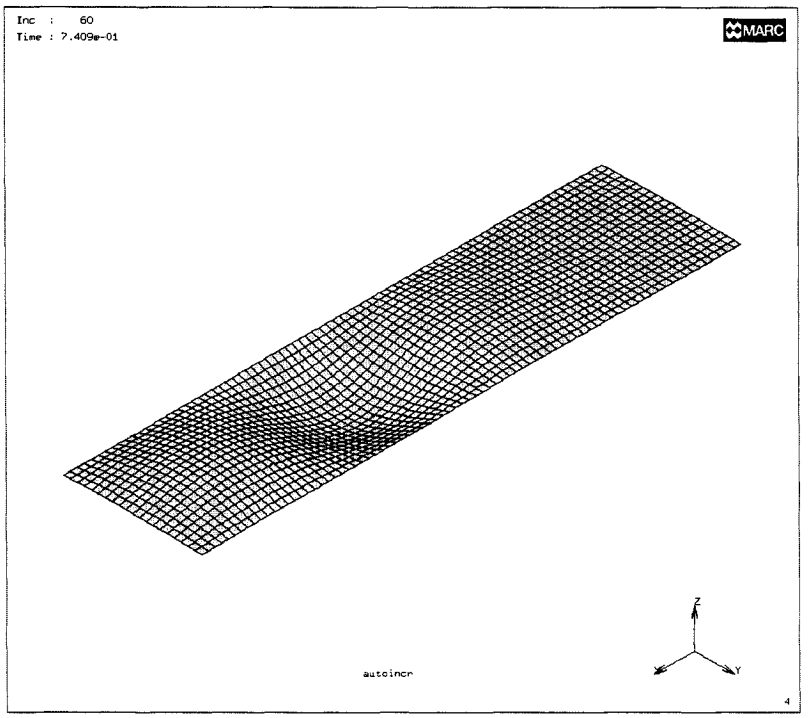


**Figure 3:** Deformed Shape of a Simply-Supported Curved Panel with $r/t$=1000, $Z_b$=5 and $a_0$=0.02 Under Compression Loading at the Post-Buckled Stage (nonlinear incremental analysis).

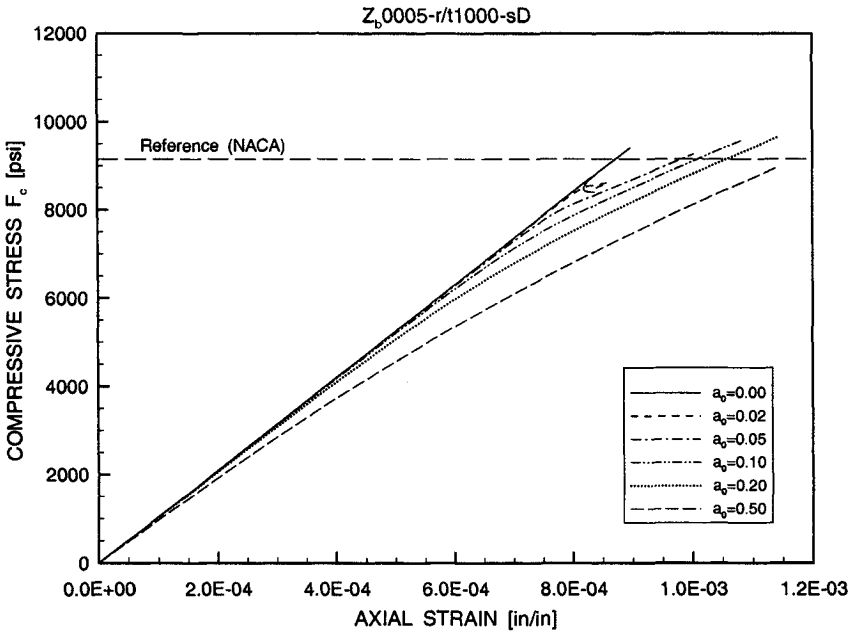


**Figure 4:** Predicted Compressive Stress-Strain Curve for a Simply-Supported Curved Panel with $r/t$=1000 and $Z_b$=5 as a Function of the Imperfection Coefficient $a_0$ (the reference buckling stress prediction based on NACA design curve is also shown [5]).

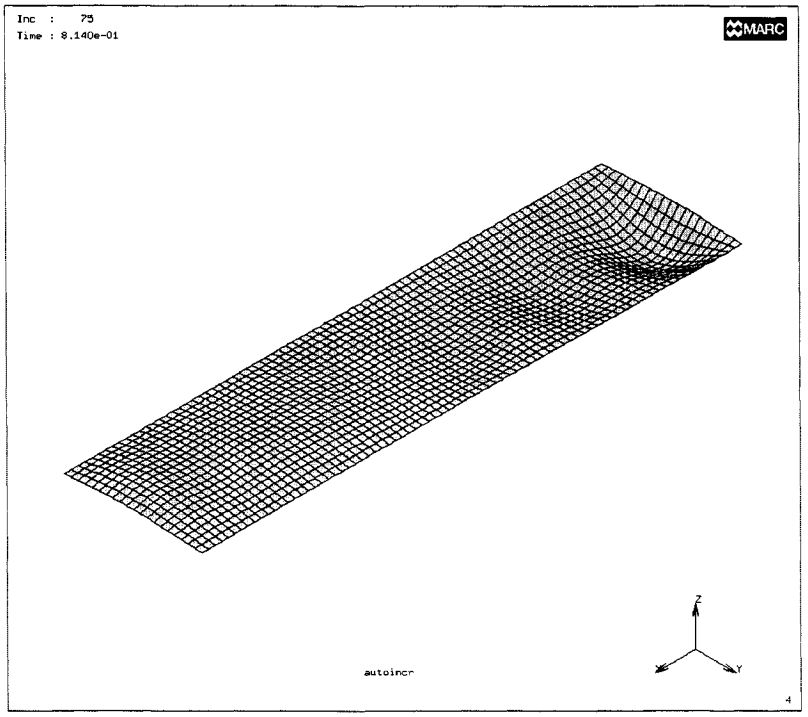


**Figure 5:** Deformed Shape of a Simply-Supported Curved Panel with $r/t$=1000, $Z_b$=30 and $a_0$=0.10 Under Compression Loading at the Post-Buckled Stage (nonlinear incremental analysis).

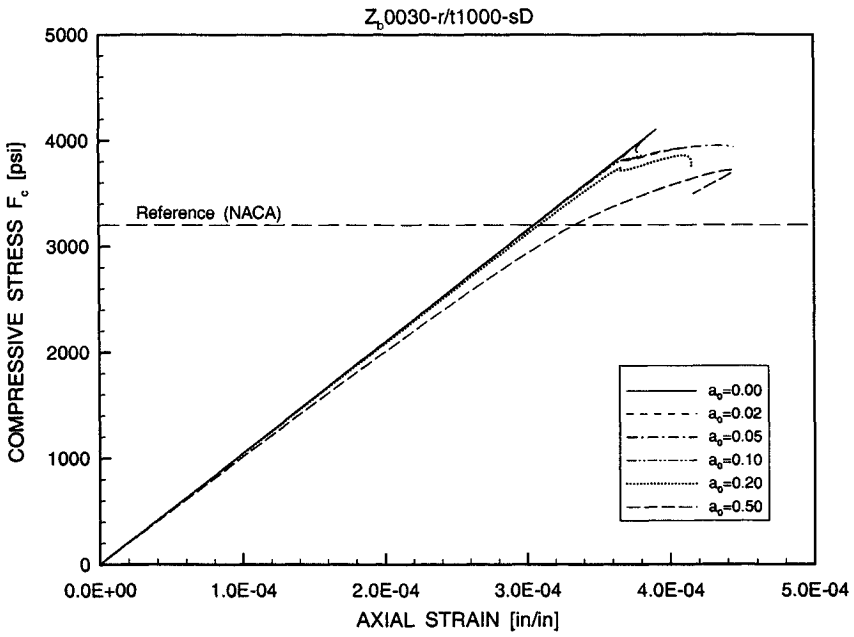


**Figure 6:** Predicted Compressive Stress-Strain Curve for a Simply-Supported Curved Panel with $r/t$=1000 and $Z_b$=30 as a Function of the Imperfection Coefficient $a_0$ (the reference buckling stress prediction based on NACA design curve is also shown [5]).

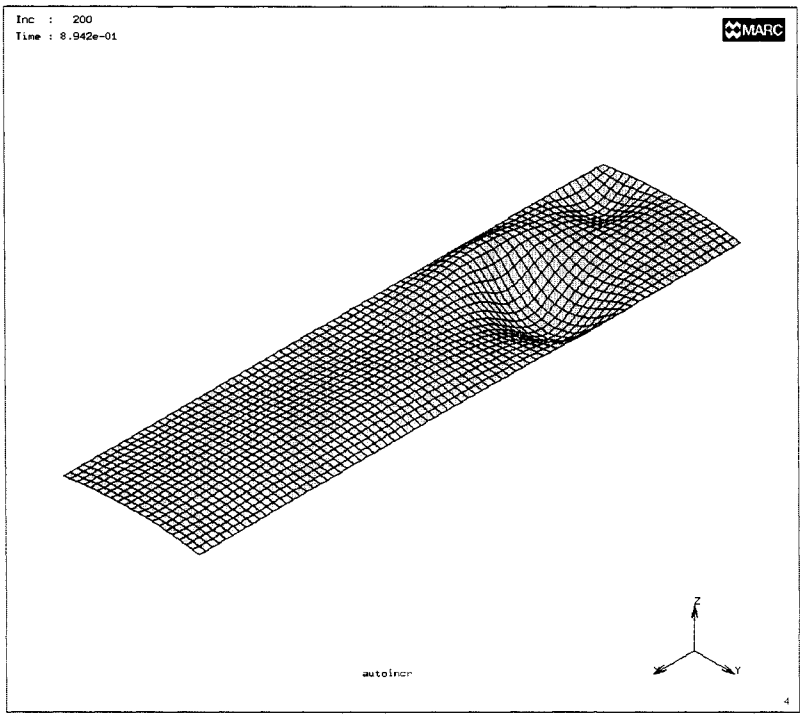


**Figure 7:** Deformed Shape of a Simply-Supported Curved Panel with $r/t$=1000, $Z_b$=100 and $a_0$=0.20 Under Compression Loading at the Post-Buckled Stage (nonlinear incremental analysis).

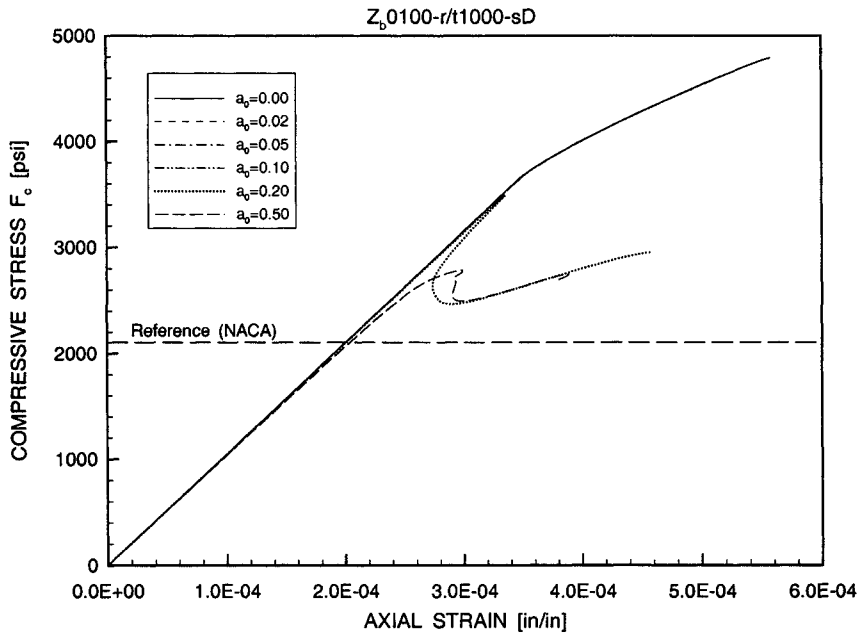


**Figure 8:** Predicted Compressive Stress-Strain Curve for a Simply-Supported Curved Panel with $r/t$=1000 and $Z_b$=100 as a Function of the Imperfection Coefficient $a_0$ (the reference buckling stress prediction based on NACA design curve is also shown [5]).

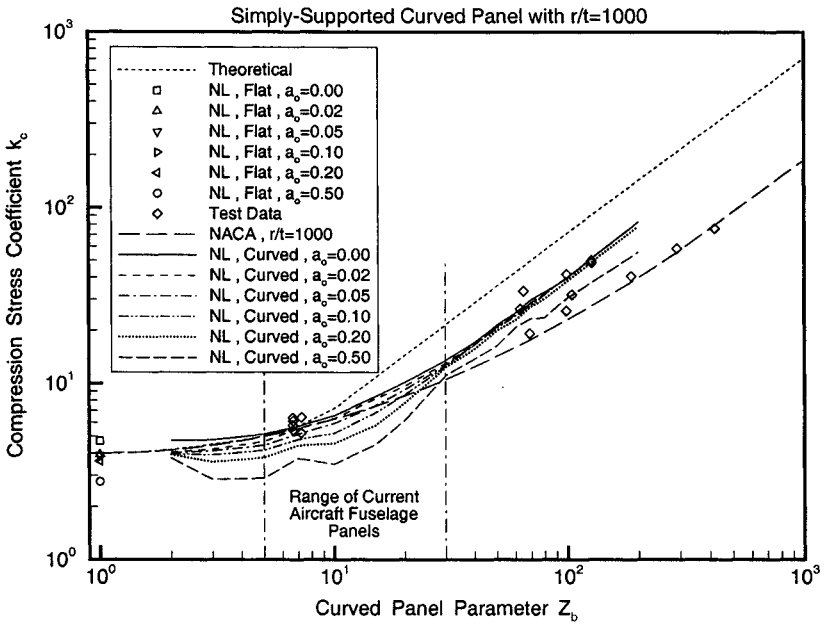


**Figure 9:** Nonlinear FEA Prediction of the Compressive Buckling Stress Coefficient $k_c$ for Simply-Supported Curved Panels with $r/t$=1000 as a Function of the Panel Parameter $Z_b$ and for Various Values of the Imperfection Coefficient $a_0$ (the Current NACA Design Curve and Several Test Points are also shown).

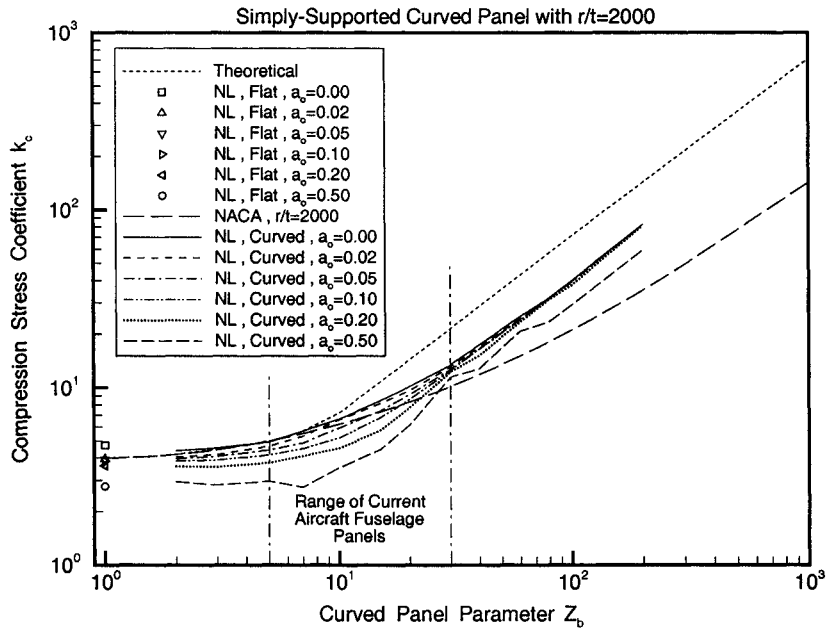


**Figure 10:** Nonlinear FEA Prediction of the Compressive Buckling Stress Coefficient $k_c$ for Simply-Supported Curved Panels with $r/t$=2000 as a Function of the Panel Parameter $Z_b$ and for Various Values of the Imperfection Coefficient $a_0$ (the Current NACA Design Curve is also shown).

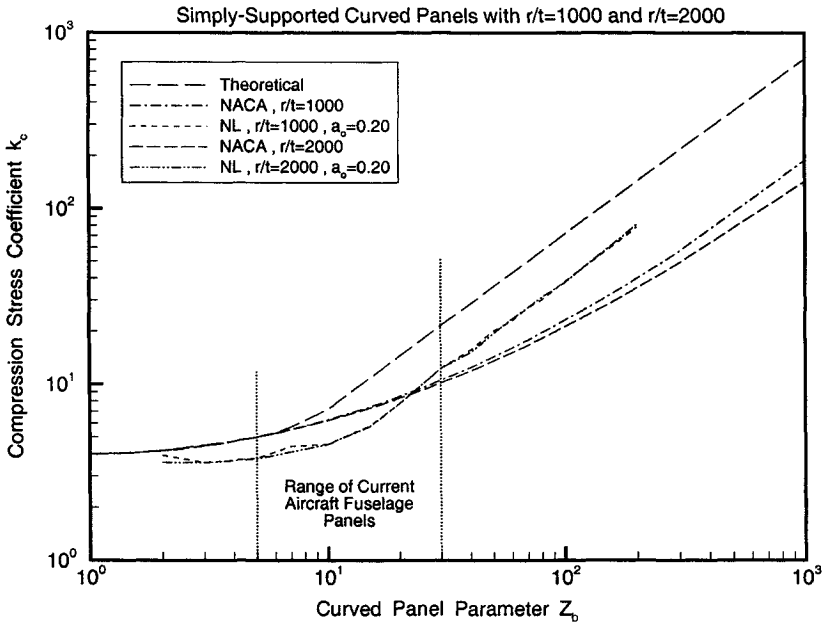


**Figure 11:** Comparison in the Predicted Compressive Buckling Stress Coefficient $k_c$ Between Simply-Supported Curved Panels with $r/t$=1000 and $r/t$=2000 for an Imperfection Coefficient of $a_0$=0.20 (the Current NACA Design Curves are also shown).

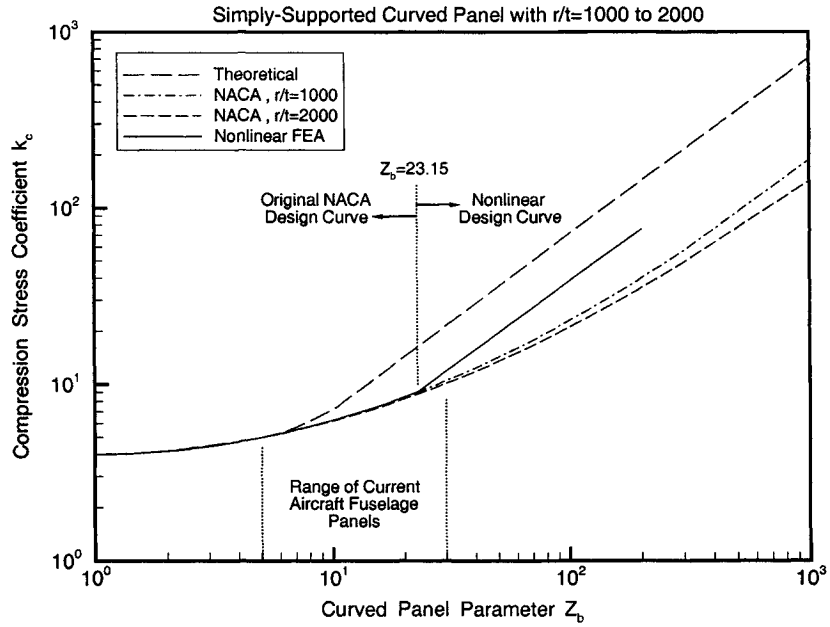


**Figure 12:** Proposed Nonlinear Design Curve for the Compressive Buckling Stress Coefficient $k_c$ for Simply-Supported Curved Panels with $1000 \le r/t \le 2000$ in the Panel Parameter Range of $1 \le Z_b \le 200$ (the Current NACA Design Curves are also shown).